New Journal of Physics
The open access journal at the forefront of physics

Deutsche Physikalische Gesellschaft DPG IOP Institute of Physics

PAPER • OPEN ACCESS

Direct writing of single germanium vacancy center arrays in diamond

To cite this article: Yu Zhou *et al* 2018 *New J. Phys.* **20** 125004

New Journal of Physics
The open access journal at the forefront of physics

Deutsche Physikalische Gesellschaft DPG
IOP Institute of Physics

Published in partnership with: Deutsche Physikalische Gesellschaft and the Institute of Physics

OPEN ACCESS

RECEIVED
31 August 2018

REVISED
14 November 2018

ACCEPTED FOR PUBLICATION
21 November 2018

PUBLISHED
14 December 2018

PAPER

Direct writing of single germanium vacancy center arrays in diamond

Yu Zhou[1], Zhao Mu[1], Giorgio Adamo[1,2], Sven Bauerdick[3], Axel Rudzinski[3], Igor Aharonovich[4,5] and Wei-bo Gao[1,2,5]

[1] Division of Physics and Applied Physics, School of Physical and Mathematical Sciences, Nanyang Technological University, Singapore 637371, Singapore
[2] The Photonics Institute and Centre for Disruptive Photonic Technologies, Nanyang Technological University, 637371 Singapore, Singapore
[3] Raith GmbH, D-44263 Dortmund, Germany
[4] Institute of Biomedical Materials and Devices (IBMD), Faculty of Science, University of Technology Sydney, Ultimo, NSW, 2007, Australia
[5] Authors to whom any correspondence should be addressed.

E-mail: Igor.Aharonovich@uts.edu.au **and** wbgao@ntu.edu.sg

Keywords: conversion yield, germanium vacancy center, single photon emitter

Abstract

Color centers in diamond are promising solid-state qubits for scalable quantum photonics applications. Amongst many defects, those with inversion symmetry are of an interest due to their promising optical properties. In this work, we demonstrate a maskless implantation of an array of bright, single germanium vacancy (GeV) centers in diamond. Employing the direct focused ion beam technique, single GeV emitters are engineered with the spatial accuracy of tens of nanometers. The single GeV creation ratio reaches as high as 53% with the dose of 200 Ge^{+} ions per spot. The presented fabrication method is promising for future nanofabrication of integrated photonic structures with GeV emitters as a leading platform for spin-spin interactions.

Single photon emitters in solid-state systems with superior optical properties are of fundamental importance for they are building block candidates of many quantum optics applications [1–3]. The ideal qubit will have a bright narrowband emission (i.e. high Debye Waller (DW) factor) and an access to optically read out and manipulate its spin states. Numerous candidates have been studied in diamond including the nitrogen vacancy (NV) center [4, 5] and more recently the silicon vacancy (SiV) center [6–10]. The advantage of the SiV is its high DW factor, with nearly 80% of its emission is within its zero phonon line (ZPL) [6]. But its coherence time is limited by the narrow ground state splitting (~40 GHz) which favors single-phonon absorption from the lower branch to the upper one [11]. This necessitates the search for an alternative system with a larger ground state splitting to suppress the phonon-mediated processes.

Recently, a new color center in diamond has been discovered, namely the GeV [12, 13]. It can be incorporated into diamond during a high pressure high temperature (HPHT) growth, or during a chemical vapor deposition (CVD) growth [14] or using ion implantation [15, 16]. It possesses a narrowband emission with a ZPL at ~602 nm. The ground state splitting of the GeV is around ~170 GHz [17] almost three times as large as SiV [18]. So far however, the coherence time in GeV was measured to be around 20 ns at 2K [17], on par or slightly lower than that of the SiV defect. The low coherence time may be a result of the changes in the orbital relaxation rate at a liquid helium temperature [19, 20]. According to the simulation in [19], at a temperature less than 1.5 K, orbital relaxation rate of GeV will be reduced, which should result in longer coherence time.

In this work we demonstrate a direct scalable fabrication of single GeV arrays in diamond produced by a focus ion beam (FIB) implantation technique. This method can result in emitter formation with spatial resolution of tens of nanometers and a creation effiency of up to 53%.

The structure of the GeV defect consists of an interstitial germanium atom splitting two adjacent vacancies in a diamond lattice, as displayed in figure 1(a). Similarly to the SiV defect, the GeV has a D_{3d} symmetry. To generate the GeV centers, ion beam implantation was employed in a commercially available 35 keV nanoFIB system (ionLINE, RAITH Nanofabrication). The whole system creates a very tightly focused Ge ion beams down

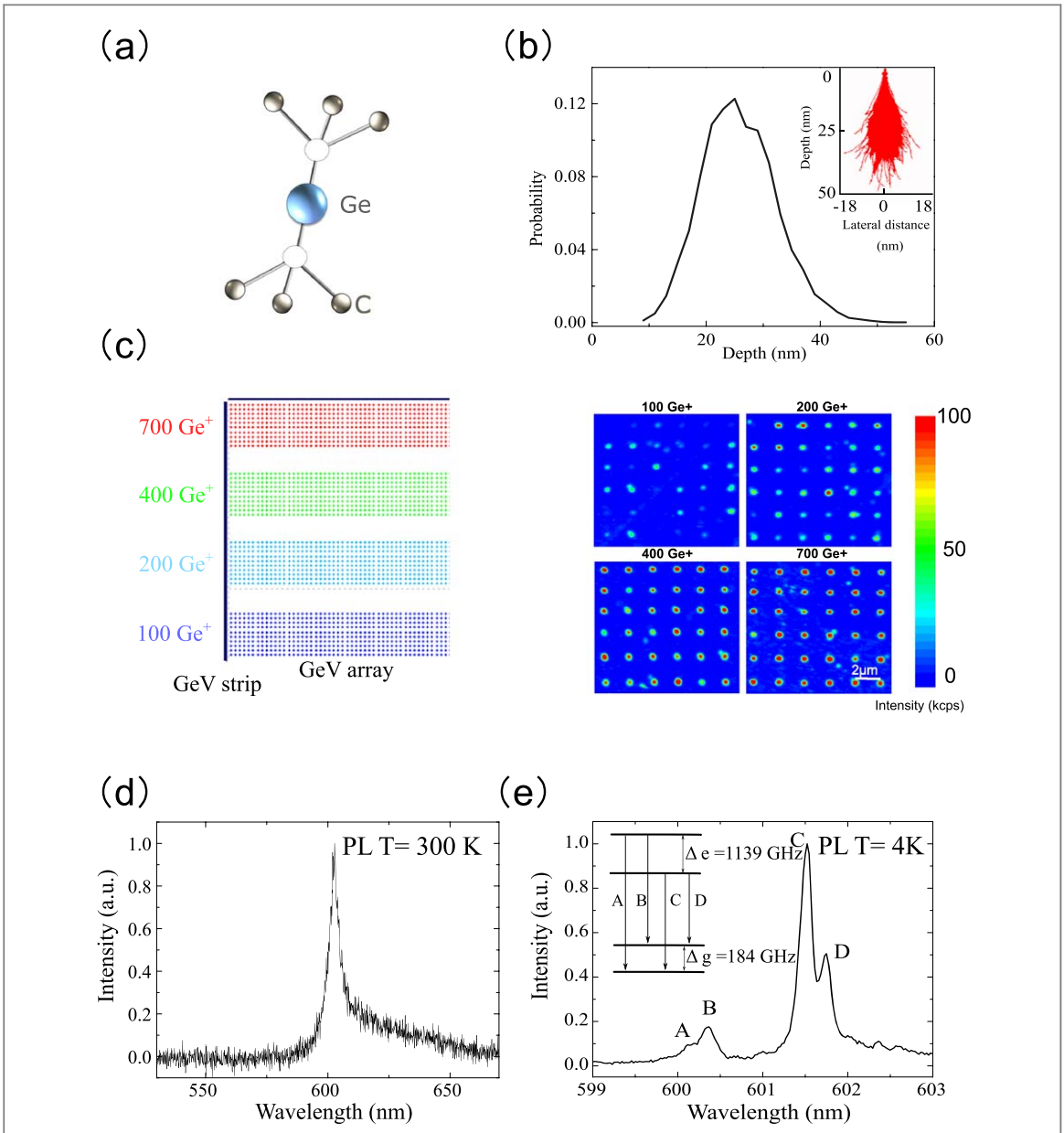

Figure 1. FIB implantation GeV ensembles. (a)Molecular structure of the GeV in diamond. (b) Depth profile from the SRIM simulation of the 35 keV Ge ions implanted into diamond. The insert figure is the simulated trajectory of 500 ions. (c) Left: designed implantation pattern with two GeV ensembles strips and arrays of four difference doses. Right: Confocal scan map of 4 different doses in the same color bar. (d) Room temperature PL spectrum of the GeV ensembles strip, ZPL is at 602 nm. (e) Cryotemperature PL spectrum of the GeV ensembles from the strip, transitions A B C D is marked and clear, and from multipeak Lorentz fitting, ground sate splitting and excited state splitting are obtained to be 184 GHz and 1139 GHz, respectively.

to a few nanometers spot size which ensures the high spatial resolution distribution of the implantation process. From the monte carlo simulation, the employed energy of 35 keV will result in Ge ions penetrating a very shallow depth of ~25 nm (figure 1(b)). The longitudinal and lateral straggling uncertainty is ~5 and ~4 nm, respectively. Considering the FIB size ~40 nm, we estimate that the spatial positioning of the ions is below 60 nm in all three dimensions [21–23].

The targeted diamond sample is a high purity CVD diamond from Element Six [N]< 1 ppb. By controlling the beam current and the dwell time we implanted Ge + with four doses (100, 200, 400, 700 Ge^+ per spot). The implantation pattern is shown in figure 1(c), two 1.5 μm wide stripes are generated by 700 Ge^+ implantations with 19 nm step size. GeV array with 4 different doses is shown using four different colors for clarity. Sites are separated by 2 μm in both directions. After the implantation, the sample was annealed at 1000 °C for 30 min in high vacuum.

The GeV color centers are characterized by home built confocal microscopy system. 532 nm laser beam was used to excite the defects through either a 100x oil immersion objective (numerical aperture 1.3) at room temperature or an air objective (numerical aperture 0.8) at 10 K . The fluorescence is collected using a single

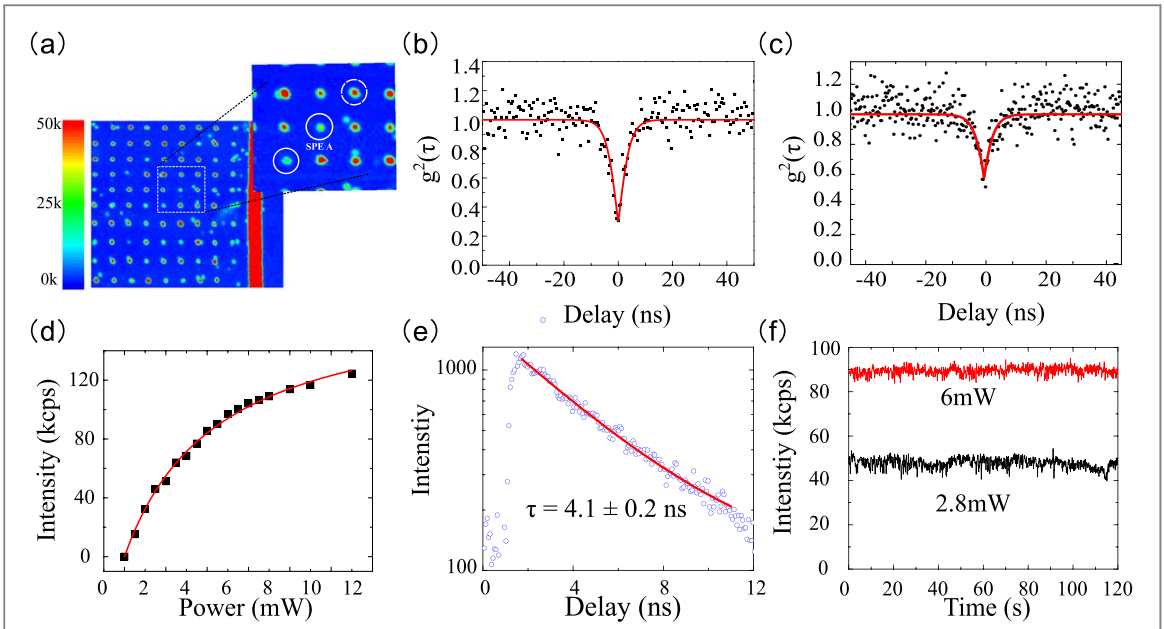

Figure 2. Single GeV center in diamond. (a) Left: Confocal scan map of 200 Ge^+ implanted area. Right: zoom in of the white dashed square part, single GeV and double GeVs are marked with solid and dashed white circle, respectively. (b) Second-order autocorrelation measurement of a single GeV center with $g^2(0) = 0.29 \pm 0.04$. (c) Second-order autocorrelation measurement of typical two GeV centers with $g^2(0) = 0.57$. (d) Saturation curve of the SPE A, the black background corrected data was fitted with $I(P) = I_\infty P/(P + P_{sat})$. (e) Lifetime measurement with 532 nm pulsed laser, the blue circles are the raw data and the red curve is the fitting with a simple exponential decay. From the fitting, we get lifetime $\tau = 4.1 \pm 0.2$ ns. (f) The single photon emission is stable without any blinking phenomenon in 2 min with excitation power at 2.8 mW and 6 mW, respectively.

mode fiber guided to either spectrometer or single photon counting modules (Excelitas). Figure 1(c) shows a confocal scan map of the 4 different doses implanted areas. To confirm the emission is indeed from the GeV centers, we measured their photoluminescence (PL) spectra at room temperature and at 10 K. The results are shown in figures 1(d), (e), respectively. At 10 K, the emission from the ZPL is split into four lines, corresponding to the splitting in the ground and excited states. Insert of figure 1(e) shows a simplified energy level diagram in which the ground and excited states are split by spin–orbit coupling, resulting in A, B, C, D transitions in the emission spectrum. Figure 1(e) confirms this four zero phonon line structure with ground state splitting $\Delta g = 184$ GHz and excited state splitting $\Delta e = 1139$ GHz which is similar to previously reported results [18].

Single GeV center was found in the 200 Ge^+ implanted region, marked as a single photon emitter (SPE) A with a white circle in the confocal map in figure 2(a). To confirm the nature of the emission, a second-order correlation function $g^2(\tau)$ of the same emitter A with a 600 $\pm$ 14 nm bandpass filter was measured. Deconvolution was made on the raw data to remove the effect of the detector's jitter. The response function of the single photon counting modules was measured by coupling a weak picosecond laser pulse into it. As shown in figure 2(b). The black dots are the raw data after the deconvolution without any background correction and the red curve is the fit with $g^2(\tau) = 1 - \alpha^*\exp(-|\tau|/\tau 1) + \beta^*\exp(-|\tau|/\tau 2)$ where τ_1 and τ_2 are the anti-bunching and bunching time constants, respectively. α and β are the fitting parameters [24–26]. From the fit, $g^2(0) = 0.29 \pm 0.04$ was obtained which is below 0.5 confirming the single photon behavior. Figure 2(c) shows an example of two GeV emitters formed in a single implantation spot, as evident from the $g^2(0) \sim 0.57$.

To study the optical properties of the implanted GeV centers further, we measured saturation and fluorescent lifetime. Figure 2(d) shows the saturation behavior (red squares represent the raw data), fit with $I(P) = I_\infty P/(P + P_{sat})$, where $I(P)$ is the intensity count rate at different excitation power P, P_{sat} is the excitation power at saturation and I_∞ is the emission at saturation. From the fit, we obtain $P_{sat} = 4.5 \pm 0.2$ mW, and $I_\infty = 178 \pm 4$ kcps. The measured lifetime (figure 2(e)) of the same emitter is $\tau = 4.1 \pm 0.2$ ns which is in a good agreement to previously reported results [18]. The emission from the GeV is stable, under 2 and 6 mW of excitation power (below and above saturation) as shown in figure 2(f) (bin size 0.1 s). Similar measurements were performed om more than 10 emitters, and no blinking or bleaching has been observed.

To estimate the conversion yield of the implatned Ge ions to opically active GeV centers, we normalize the fluorescence intensity of the implanted spots to the intensity of a single and double emitter reported earlier. We scanned 90 spots in each of the four implanted dose areas. The confocal maps are shown in figure 1(c). Figure 3(a) displays the analysis of the distribution of the number of emitters in each spot of the 4 implantation doses. For the 100 Ge^+ implanted area, ten out of the 36 implantation spots are dim, with no formed emitters. When the implantation dose increases to 200 Ge^+ per spot, single GeV centers are predominantly observed. A

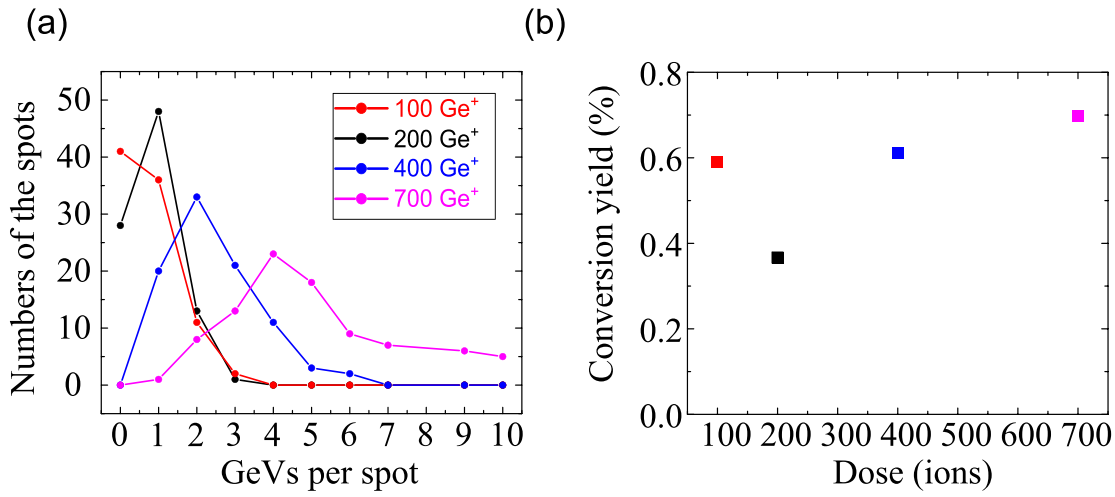

Figure 3. (a) Distribution of number of emitters in each spot of 4 different implanted doses, 90 emitters in each dose have been counted. (b) Calculated conversion yield of the 4 different implanted doses.

Table 1. Summary and comparison of generation of three difference color centers with FIB technique.

	SiV in Slicon Carbide [26]	SiV in Diamond [27]	GeV in diamond (our work)
Implantation energy	35 keV	60 keV	35 keV
Emitter conversion yield (%)	1.4–4.2	15	0.4–0.7
Single photon creation ratio (%)	38	13.3	53.33

probability of 53% is estimated to have a single emitter in an implantation spot. If the dose further increases to 400 Ge^+ or 700 Ge^+ per spot, most of the spots will contain two or more GeV centers. The conversion yield is calculated by the ratio of the numbers of emitters in each spot over the implantation dose. The results are shown in figure 3(b). As the implantation dose increases from 100 Ge^+ to 700 Ge^+ per spot, the conversion yield remains around 0.6%. This result is consistent with previous observations for SiV in silicon carbide [24], SiV in diamond [27], and on par with nitrogen implantation into diamond [28, 29]. We have summarized the previous results of generation of SiV in silicon carbide, SiV in diamond and the studied here GeV in diamond with FIB technique in table 1. Formation of SiV in diamond has the highest conversion yield of 15% and the lowest single photon creation ratio (13.3%). On the other hand, the single photon creation ratio of GeV centers in diamond can reach up to 53.33% at the dose of 200 Ge^+. This is extremely helpful in efficient and deterministic farbrication of single GeV centers at tens of nanometer spatial precision. The conversion yield can be further increased by performing high energy electron irradiation, or higher temperature annealing process [21, 24].

To conclude, we demonstrated a maskless, targeted fabrication of single germanium center arrays in diamond. From PL measurement at both room temperature and cryotemperature, we confirmed that defects are germanium vacancy center. While the conversion yield is low at this point, this can be circumvented by employing larger implantation doses or other proven methods such as high temperature annealing and electron irradiation. More significantly, with the demonstrated technique, the GeV can be positioned with a nanometer-scale spatial accuracy which will greatly benefit various of photonic structures such as photonic nano cavities [30–32] and waveguides [22, 33]. Another possible direction is that this method can help generate coupled electron spins in germanium center as well as provide a platform to achieve entanglement between spins on the condition that the coherence time of GeV centers could be further enhanced.

Acknowledgments

We thank Evan Toh and Andrew Yu for the discussion about nanofabrication. We acknowledge the support from Singapore National Research Foundation through a Singapore 2015 NRF fellowship grant (NRF-NRFF2015-03), its Competitive Research Program (CRP Award No. NRF-CRP14-2014-02), A*STAR QTE Project and Singapore Ministry of Education tier 2 project MOE2016-T2-2-077, MOE2017-T2-1-163 and tier 3 project MOE2016-T3-1-006 (S). Financial support from the Australian Research Council (via

DP180100077), the Asian Office of Aerospace Research and Development grant (FA2386-17-1-4064) and Office of Naval Research Global (N62909-18-1-2025) is acknowledged.

References

[1] Aharonovich I, Englund D and Toth M 2016 Solid-state single-photon emitters *Nat. Photonics* **10** 631–41
[2] Atatüre M, Englund D, Vamivakas N, Lee S-Y and Wrachtrup J 2018 Material platforms for spin-based photonic quantum technologies *Nat. Rev. Mater.* **3** 38–51
[3] Awschalom D D, Hanson R, Wrachtrup J and Zhou B B 2018 Quantum technologies with optically interfaced solid-state spins *Nat. Photonics* **12** 516
[4] Doherty M W, Manson N B, Delaney P, Jelezko F, Wrachtrup J and Hollenberg L C L 2013 The nitrogen-vacancy colour centre in diamond *Phys. Rep.* **528** 1–45
[5] Maurer P C, Kucsko G, Latta C, Jiang L, Yao N Y, Bennett S D, Pastawski F, Hunger D, Chisholm N and Markham M 2012 Room-temperature quantum bit memory exceeding one second *Science* **336** 1283–6
[6] Neu E, Steinmetz D, Riedrich-Möller J, Gsell S, Fischer M, Schreck M and Becher C 2011 Single photon emission from silicon-vacancy colour centres in chemical vapour deposition nano-diamonds on iridium *New J. Phys.* **13** 025012
[7] Müller T, Hepp C, Pingault B, Neu E, Gsell S, Schreck M, Sternschulte H, Steinmüller-Nethl D, Becher C and Atatüre M 2014 Optical signatures of silicon-vacancy spins in diamond *Nat. Commun.* **5** 3328
[8] Becker J N, Pingault B, Groß D, Gündoğan M, Kukharchyk N, Markham M, Edmonds A, Atatüre M, Bushev P and Becher C 2018 All-optical control of the silicon-vacancy spin in diamond at millikelvin temperatures *Phys. Rev. Lett.* **120** 053603
[9] Sukachev D D, Sipahigil A, Nguyen C T, Bhaskar M K, Evans R E, Jelezko F and Lukin M D 2017 Silicon-vacancy spin qubit in diamond: a quantum memory exceeding 10 ms with single-shot state readout *Phys. Rev. Lett.* **119** 223602
[10] Zhou Y, Rasmita A, Li K, Xiong Q, Aharonovich I and Gao W-B 2017 Coherent control of a strongly driven silicon vacancy optical transition in diamond *Nat. Commun.* **8** 14451
[11] Pingault B, Jarausch D D, Hepp C, Klintberg L, Becker J N, Markham M, Becher C and Atatüre M 2017 Coherent control of the silicon-vacancy spin in diamond *Nat. Commun.* **8** 1–7
[12] Palyanov Y N, Kupriyanov I N, Borzdov Y M and Surovtsev N V 2015 Germanium: a new catalyst for diamond synthesis and a new optically active impurity in diamond *Sci. Rep.* **5** 14789
[13] Iwasaki T *et al* 2015 Germanium-vacancy single color centers in diamond *Sci. Rep.* **5** 12882
[14] Bray K, Regan B, Trycz A, Previdi R, Seniutinas G, Ganesan K, Kianinia M, Kim S and Aharonovich I 2018 Single crystal diamond membranes containing germanium vacancy color centers arXiv:1804.02130
[15] Ekimov E A, Lyapin S, Boldyrev K N, Kondrin M V, Khmelnitskiy R, Gavva V A, Kotereva T Y V and Popova M N 2015 Germanium–vacancy color center in isotopically enriched diamonds synthesized at high pressures *JETP Lett.* **102** 701–6
[16] Palyanov Y N, Kupriyanov I N, Borzdov Y M, Khokhryakov A F and Surovtsev N V 2016 High-pressure synthesis and characterization of Ge-doped single crystal diamond *Cryst. Growth Des.* **16** 3510–8
[17] Siyushev P, Metsch M H, Ijaz A, Binder J M, Bhaskar M K, Sukachev D D, Sipahigil A, Evans R E, Nguyen C T and Lukin M D 2017 Optical and microwave control of germanium-vacancy center spins in diamond *Phys. Rev.* B **96** 081201
[18] Bhaskar M K, Sukachev D D, Sipahigil A, Evans R E, Burek M J, Nguyen C T, Rogers L J, Siyushev P, Metsch M H and Park H 2017 Quantum nonlinear optics with a germanium-vacancy color center in a nanoscale diamond waveguide *Phys. Rev. Lett.* **118** 223603
[19] Iwasaki T, Miyamoto Y, Taniguchi T, Siyushev P, Metsch M H, Jelezko F and Hatano M 2017 Tin-vacancy quantum emitters in diamond *Phys. Rev. Lett.* **119** 253601
[20] Thiering G and Gali A 2018 *Ab initio* magneto-optical spectrum of group-IV vacancy color centers in diamond *Phys. Rev.* X **8** 021063
[21] Schröder T *et al* 2017 Scalable focused ion beam creation of nearly lifetime-limited single quantum emitters in diamond nanostructures *Nat. Commun.* **8** 1–7
[22] Sipahigil A, Evans R E, Sukachev D D, Burek M J, Borregaard J, Bhaskar M K, Nguyen C T, Pacheco J L, Atikian H A and Meuwly C 2016 An integrated diamond nanophotonics platform for quantum optical networks *Science* **354** 847
[23] Burek M J, Meuwly C, Evans R E, Bhaskar M K, Sipahigil A, Meesala S, Machielse B, Sukachev D D, Nguyen C T and Pacheco J L 2017 Fiber-coupled diamond quantum nanophotonic interface *Phys. Rev. Appl.* **8** 024026
[24] Wang J, Zhang X, Zhou Y, Li K, Wang Z, Peddibhotla P, Liu F, Bauerdick S, Rudzinski A and Liu Z 2017 Scalable fabrication of single silicon vacancy defect arrays in silicon carbide using focused ion beam *ACS Photonics* **4** 1054–9
[25] Kurtsiefer C, Mayer S, Zarda P and Weinfurter H 2000 Stable solid-state source of single photons *Phys. Rev. Lett.* **85** 290
[26] Radulaski M, Widmann M, Niethammer M, Zhang J L, Lee S-Y, Rendler T, Lagoudakis K G, Son N T, Janzen E and Ohshima T 2017 Scalable quantum photonics with single color centers in silicon carbide *Nano Lett.* **17** 1782–6
[27] Tamura S *et al* 2014 Array of bright silicon-vacancy centers in diamond fabricated by low-energy focused ion beam implantation *Appl. Phys. Express* **7** 115201
[28] Toyli D M, Weis C D, Fuchs G D, Schenkel T and Awschalom D D 2010 Chip-scale nanofabrication of single spins and spin arrays in diamond *Nano Lett.* **10** 3168–72
[29] Meijer J, Burchard B, Domhan M, Wittmann C, Gaebel T, Popa I, Jelezko F and Wrachtrup J 2005 Generation of single color centers by focused nitrogen implantation *Appl. Phys. Lett.* **87** 261909
[30] Faraon A, Santori C, Huang Z, Acosta V M and Beausoleil R G 2012 Coupling of nitrogen-vacancy centers to photonic crystal cavities in monocrystalline diamond *Phys. Rev. Lett.* **109** 033604
[31] Riedrich-Möller J, Arend C, Pauly C, Mücklich F, Fischer M, Gsell S, Schreck M and Becher C 2014 Deterministic coupling of a single silicon-vacancy color center to a photonic crystal cavity in diamond *Nano Lett.* **14** 5281–7
[32] Zhang J L, Sun S, Burek M J, Dory C, Tzeng Y-K, Fischer K A, Kelaita Y, Lagoudakis K G, Radulaski M and Shen Z-X 2018 Strongly cavity-enhanced spontaneous emission from silicon-vacancy centers in diamond *Nano Lett.* **18** 1360–5
[33] Lemonde M-A, Meesala S, Sipahigil A, Schuetz M, Lukin M, Loncar M and Rabl P 2018 Phonon networks with silicon-vacancy centers in diamond waveguides *Phys. Rev. Lett.* **120** 213603